Text S1. Methods

1.1. Autonomous Ferry Observations

The Ocean Networks Canada (ONC) monitoring system stationary, cabled, and ferry-based instruments currently deploys hundreds of instruments that total thousands of sensors, and collectively relay hundreds of Gigabytes per day and >1 PB of uncompressed data to the Oceans data platform (Owens et al. 2022). For our work, the high-resolution FerryBox observations were averaged every minute and therefore were in near equal proportion from the thermosalinograph ($n_{thermosalin}$= 173,522) and fluorometer ($n_{fluorometer}$= 173,356). Additional hardware attributes of the HoloSea S7 holographic microscope include that its 15 mm sample space was oriented perpendicular with water intake below an output line to ensure steady flow. When filled with water, the microscope and chamber total ~22 kg. Regarding software, further information on the efficient numerical wavefront reconstructions from inline holographic microscopes are available (e.g., Kanka *et al.* 2009).

High resolution bathymetry (Figure 1) downloaded from GEBCO gridded global terrain model (2023)[1] and the coastline shapefiles from the British Columbia data catalogue[2]. All data analysis was conducted in the R programming language (R Core Team 2022). A broad set of cleaning operations for data filtering and arranging were completed using the *tidyverse* (v. 2.0.0; Wickham et al. 2019). FerryBox data were aggregated to minute averages using *timek* package (v. 2.8.3; Dancho 2022). All spatiotemporal ferry observations were transformed to spatial vector data in the *sf* package (v. 1.0.9; Pebesma 2018). To construct Hovmöller diagrams from FerryBox data, all spatial vectors for each time point were rasterized and stacked in the *raster* package (v. 3.6.14; Hijmans 2021), finally supplied to Hovmöller constructor in the *rasterVis* package (v. 0.5.15; Lamigueiro 2022). The loess smoothing approximation (Figure S8) used the *latticeExtra* package (v. 0.6.29; Sarkar & Andrews, 2022).

[1] https://www.gebco.net/data_and_products/gridded_bathymetry_data/

[2] https://catalogue.data.gov.bc.ca/dataset/nts-bc-coastline-polygons-1-250-000-digital-baseline-mapping-nts

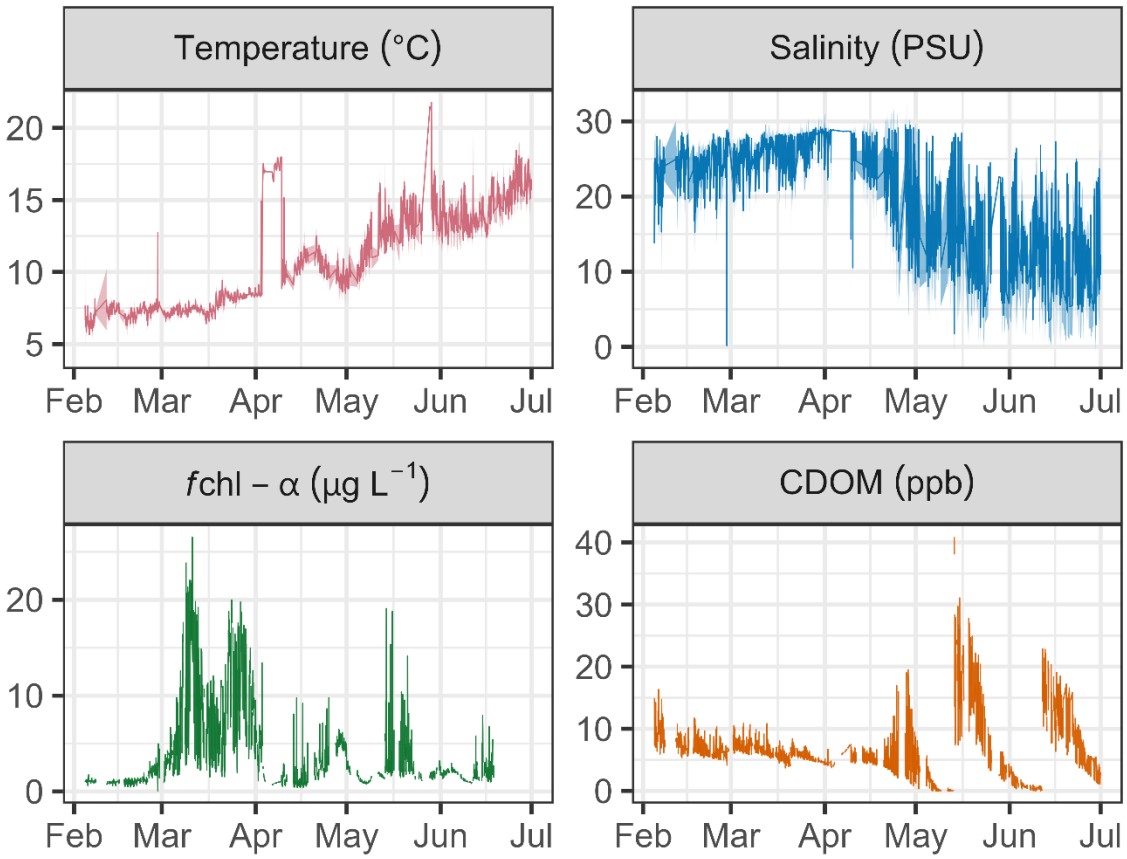

Figure S1. FerryBox record February-June 2020 down sampled and plotted as median values (bold line) with minimum and maximum intervals from a box car resampling algorithm requiring 70% data availability using Ocean Networks Canada's Oceans 2.0-3.0 Data Portal[3]. Temperature and salinity derive from a Seabird thermosalinograph and fluorescence values of chlorophyll and chromophoric dissolved organic matter (CDOM) are produced by fluorometer manifold (See Table S2 for instrument details and calibration records). Seasonal patterns are evident here showing spring warming initiated in April, preceded by a spring bloom with minor CDOM values, likely supporting high autotrophic growth through high light availability. The Fraser River freshet begins in May and peaks in June, injecting substantial freshwater into the Strait and raising CDOM concentrations with terrestrial particulates. Anomalously high chlorophyll and CDOM concentrations in June likely indicate instrument fouling under high sediment inputs from the Fraser River. Vertical interruptions in instrument readings indicate cleaning and refurbishment periods.

[3] https://data.oceannetworks.ca/home

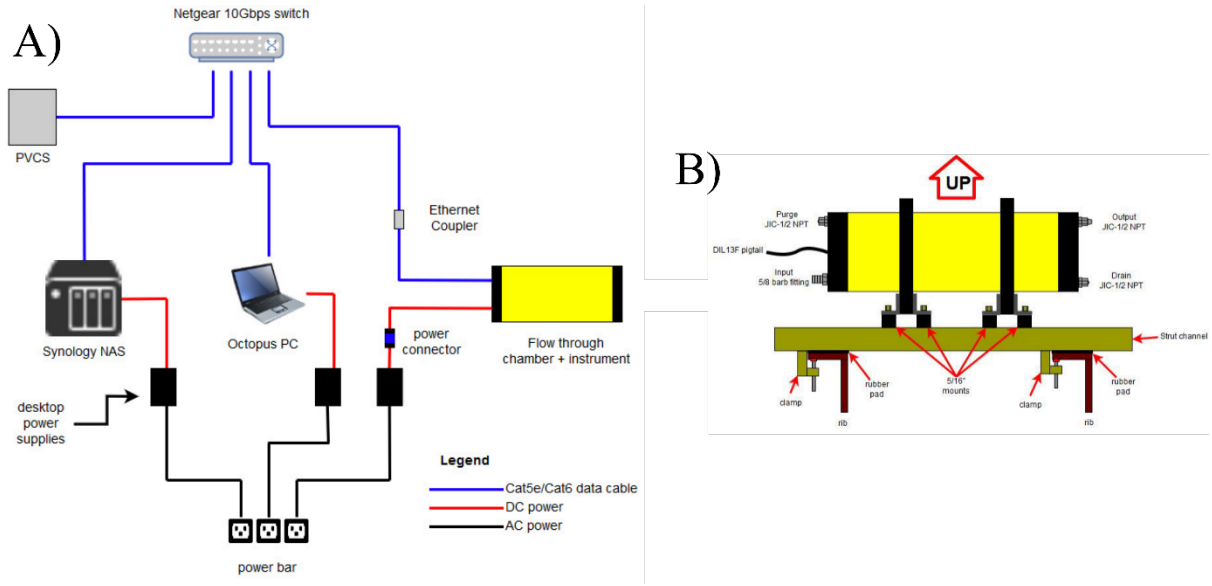

Figure S2. A) Networked components (PVCS; Pump and Valve Control System) for holographic imaging support image collection and storage for the B) data taken by the microscope from flow-through sampling (Developed by Ian Beliveau). See Owens et al. (2022) for more details on system topology and features for automatic data storage and database integration. Selected sampling days after holographic microscope cleaning are shown in Table S3.

Table S1. Description references for major plankton taxa including broad taxonomic group and genus where available.

Taxonomic group	Genera	Description reference
Copepods	NA	Conway (2006)
Ciliophora	NA	Dolan (2013)
Centric diatom	*Chaetoceros*	Hasle & Syvertsen (1997)
	Ditylum	Hasle & Syvertsen (1997)
	Eucampia	Hasle & Syvertsen (1997)
	Odontella	Hasle & Syvertsen (1997)
	Proboscia	Hasle & Syvertsen (1997)
	Skeletonema	Hasle & Syvertsen (1997)
	Thalassiosira	Hasle & Syvertsen (1997)
Pennate diatom	*Cylindrotheca*	Hasle & Syvertsen (1997)
	Nitzschia	Hasle & Syvertsen (1997)
Diatom	*Thalassionema*	Hasle & Syvertsen (1997)
Dinoflagellate	*Tripos* (*Neoceratium*)	Steidinger & Jangen (1997), Gómez (2013)
	Tripos fusus	Steidinger & Jangen (1997), Gómez (2013)
	Tripos lineatum	Steidinger & Jangen (1997), Gómez (2013)
	Prorocentrum	Steidinger & Jangen (1997)
	Gyrodinium	Steidinger & Jangen (1997)
Silicoflagellates	*Dictyocha*	Throndsen (1997)

Table S2. Transect image dataset, where asterisks (*) indicate cleaning date of microscope lens and casing along with data swap from a network-accessed storage device. During cleaning, fouling was removed, the microscope flow-through chamber was drained into the bilge and the microscope was removed to clean the casing and lens. Volume estimates are based on effective image volume calculated in Walcutt et al. 2020).

Date	Time	Departure	Transects	Holograms	Volume (mL)
2020-02-25*	20:50-22:30	Tsawwassen	1	5000	315
2020-02-26	20:50-22:30	Tsawwassen	1	5000	315
2020-02-27	20:50-22:30	Tsawwassen	1	5000	315
2020-02-28	20:50-22:30	Tsawwassen	1	5000	315
2020-03-20*	19:50-21:30	Duke Point	1	5000	315
2020-03-21	19:50-21:30	Duke Point	1	5000	315
2020-03-22	19:50-21:30	Duke Point	1	5000	315
2020-03-23	19:50-21:30	Duke Point	1	4800	302
2020-04-09*	20:00-21:30	Duke Point	1	3700	233
2020-04-10	19:50-21:30	Duke Point	1	4500	284
2020-04-14	17:30-21:30	Tsawwassen	1	5123	323
2020-04-15	19:50-23:00	Duke Point	1	5007	315
2020-04-16	19:50-00:00	Duke Point	2	10600	668

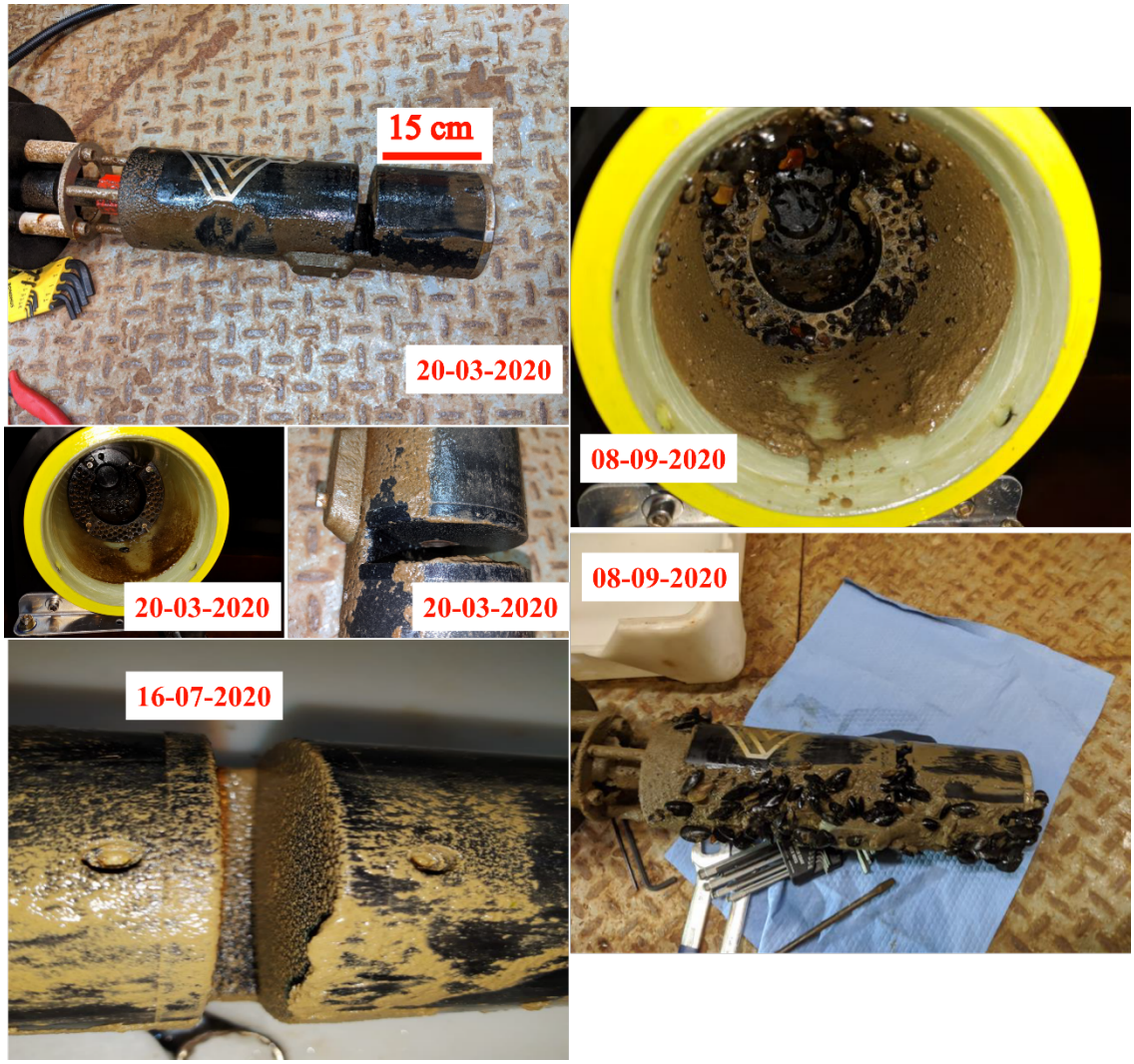

Figure S3. Fouling condition of the HoloSea during cleaning visits by the Marine Technology Centre of Ocean Networks Canada. Red scale bar indicates ~15 cm. Fouling was sediment-based and relatively mild in March however photos clearly reflect intense fouling in July cumulatively built from the Fraser River Freshet. Fouling intensified further through summer and autumn, showing persistent mussel colonization on the instrument and inside the flow-through chamber. Interruptions in regular cleaning due to COVID-19 ferry regulations were key impediments to data quality in summer and autumn.

Table S3. Estimated biofouling effect on the WET Labs ECO Triplet fluorometer approximated as the difference in fluorescence of a standardized solution (™ Diet Coke) before and after cleaning (e.g. Wang et al. 2019).

Cleaning Intervals	% Change per day
2020-02-11 — 2020-02-25	-0.07
2020-02-25 — 2020-03-20	-1.22
2020-03-20 — 2020-04-09	-2.17
2020-04-09 — 2020-05-13	-2.42
2020-05-13 — 2020-06-11	-2.95
2020-06-11 — 2020-06-18	-1.32

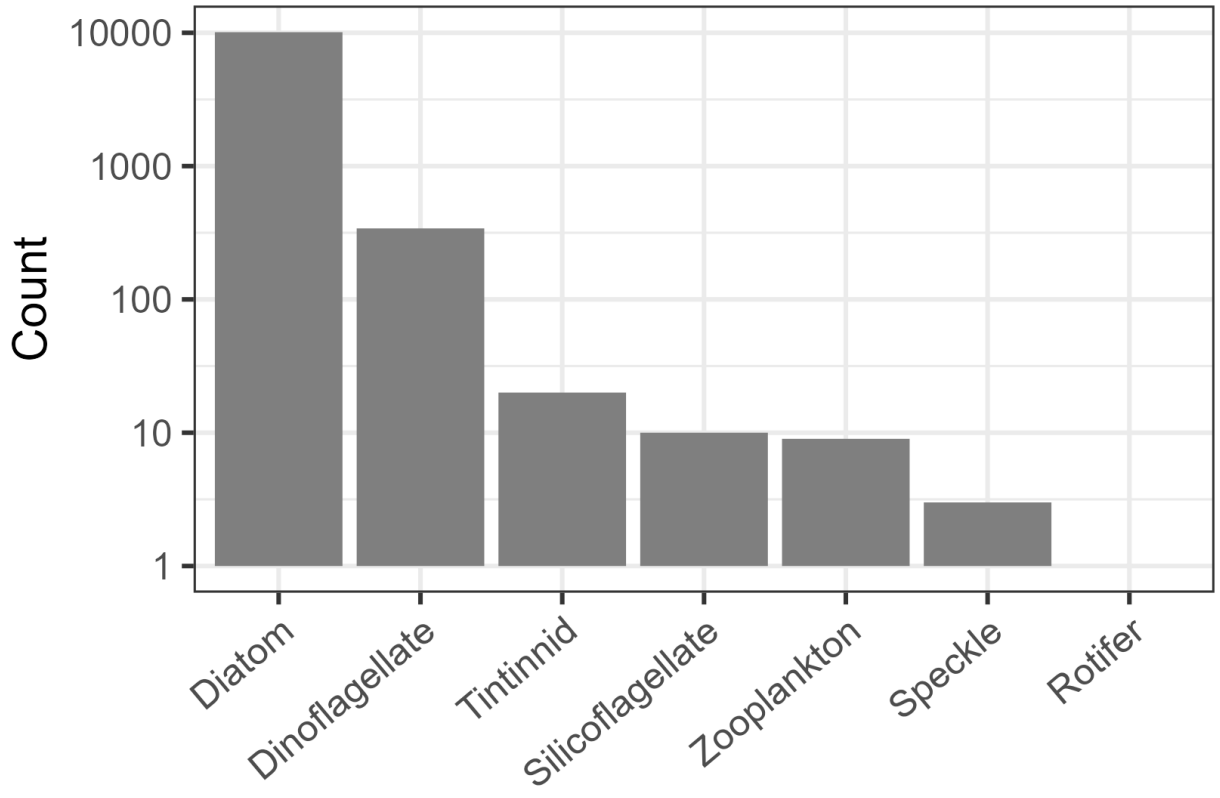

Figure S4. The frequency count of each major group identified in holograms, defined with a log-scale y-axis. The speckle category incorporates a common type of noise produced by digital holography (Garcia-Sucerquia et al. 2005).

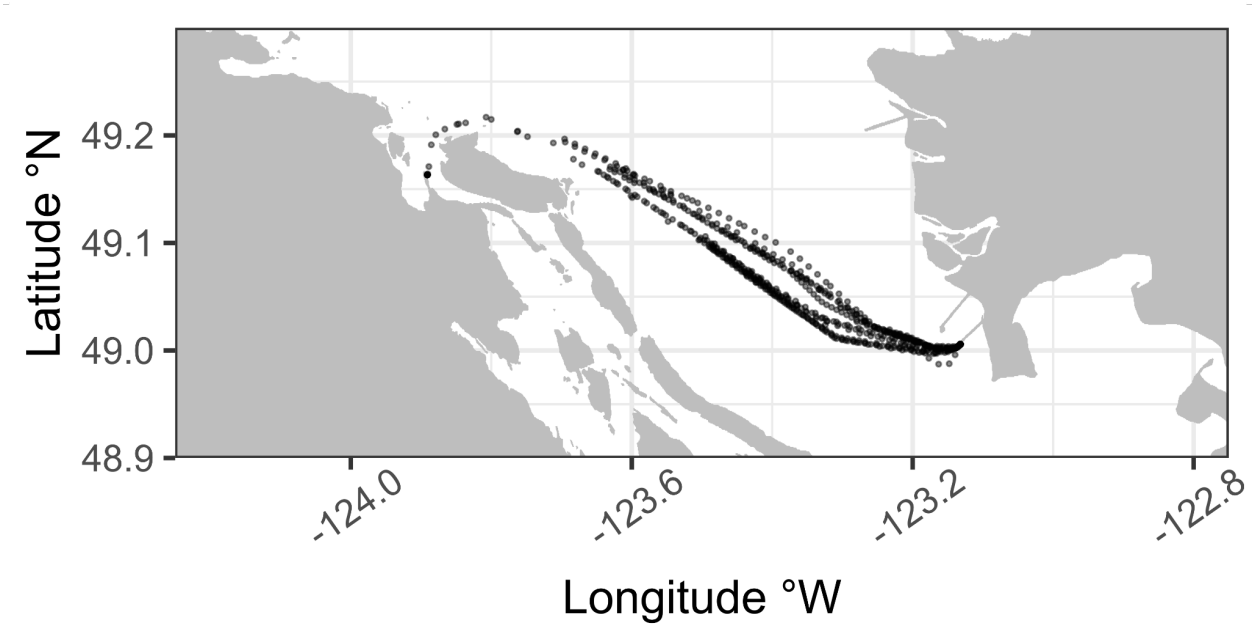

Figure S5. Spatial coverage of holographic imaging points. Due to limited cleaning access, imaging samples from February-March cluster to the eastward side of the Strait of Georgia.

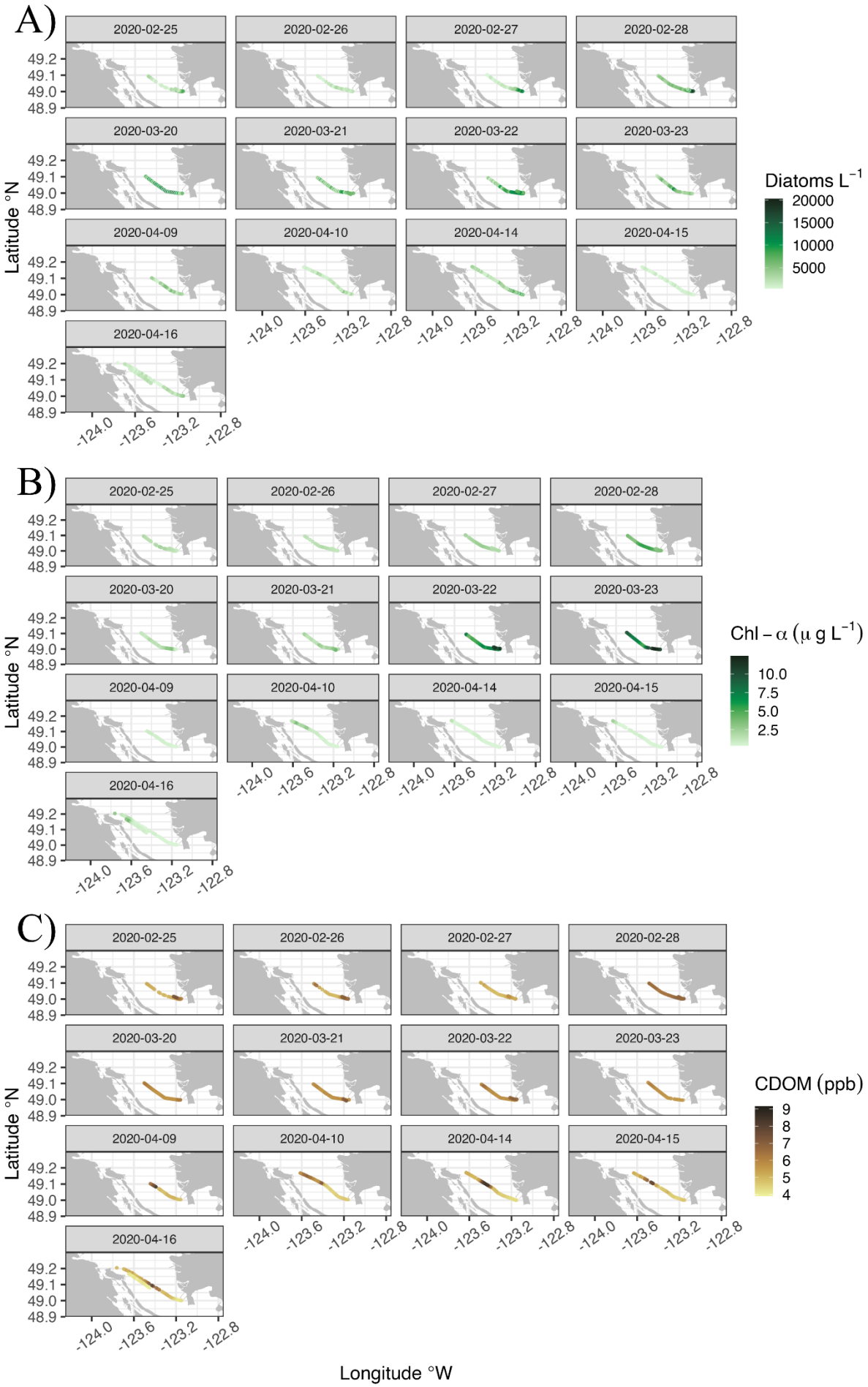
A)
2020-02-25
2020-02-26
2020-02-27
2020-02-28
2020-03-20
2020-03-21
2020-03-22
2020-03-23
2020-04-09
2020-04-10
2020-04-14
2020-04-15
2020-04-16
Latitude °N
49.2
49.1
49.0
48.9
-124.0
-123.6
-123.2
-122.8
Diatoms L^{-1}
20000
15000
10000
5000
B)
Chl – α (μ g L^{-1})
10.0
7.5
5.0
2.5
C)
CDOM (ppb)
9
8
7
6
5
4
Longitude °W

Figure S6. Daily transect coverage for holographic imaging with corresponding A) diatom concentrations and B) chlorophyll-α fluorescence (*f*chl-α) at each point. As holographic imaging initiates once per day usually near dusk, and usually from Tsawwassen terminal (Table S2), sampling is clustered on the eastward side of the Strait. The imaging transects in February occur 1-2 weeks prior to the spring bloom, after its peak in March, and at the onset of spring warming and freshening in the Strait (Figure S8). This also provides limited evidence to support the spatial structuring of plankton blooms, where higher *f*chl-α and diatom concentrations tend towards the east and westward sections of the strait, especially during the freshet period (April), where the influence of the Fraser River in suppressing light availability peaks.

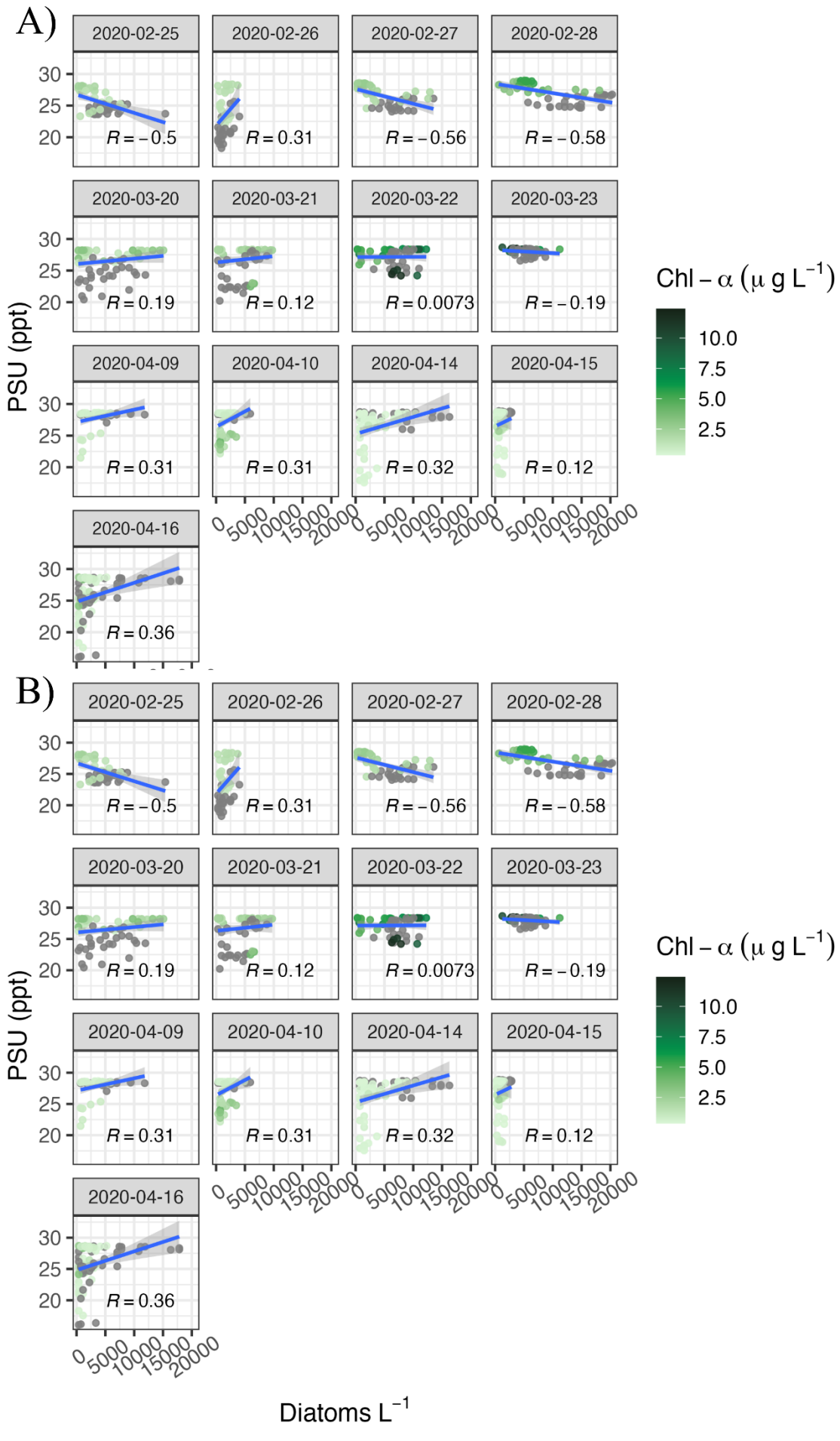
A)
2020-02-25
2020-02-26
2020-02-27
2020-02-28
R = −0.5
R = 0.31
R = −0.56
R = −0.58
2020-03-20
2020-03-21
2020-03-22
2020-03-23
R = 0.19
R = 0.12
R = 0.0073
R = −0.19
2020-04-09
2020-04-10
2020-04-14
2020-04-15
R = 0.31
R = 0.31
R = 0.32
R = 0.12
2020-04-16
R = 0.36
PSU (ppt)
30
25
20
0
5000
10000
15000
20000
Chl − α (μ g L−1)
10.0
7.5
5.0
2.5
B)
Diatoms L−1

Figure S7. Linear correlations between holographic cell concentrations (Cells L^{-1}) and A) salinity (PSU) and B) chromophoric dissolved organic matter (CDOM) shows mixed relationships until April and the onset of the Fraser River freshet. Here, more saline, less turbid waters are associated with higher cell concentrations, whereas fresher turbid waters– signifying strong seasonal inputs from the Fraser River are associated with lower cell concentrations. This pattern fits the described process whereby diminished light availability in the river-borne plume waters suppresses light availability and planktonic productivity (Yin et al. 1997). Points are filled with *f*chl-α values and where missing readings colored grey; no clear pattern relates *f*chl-α to these complex physicochemical conditions.

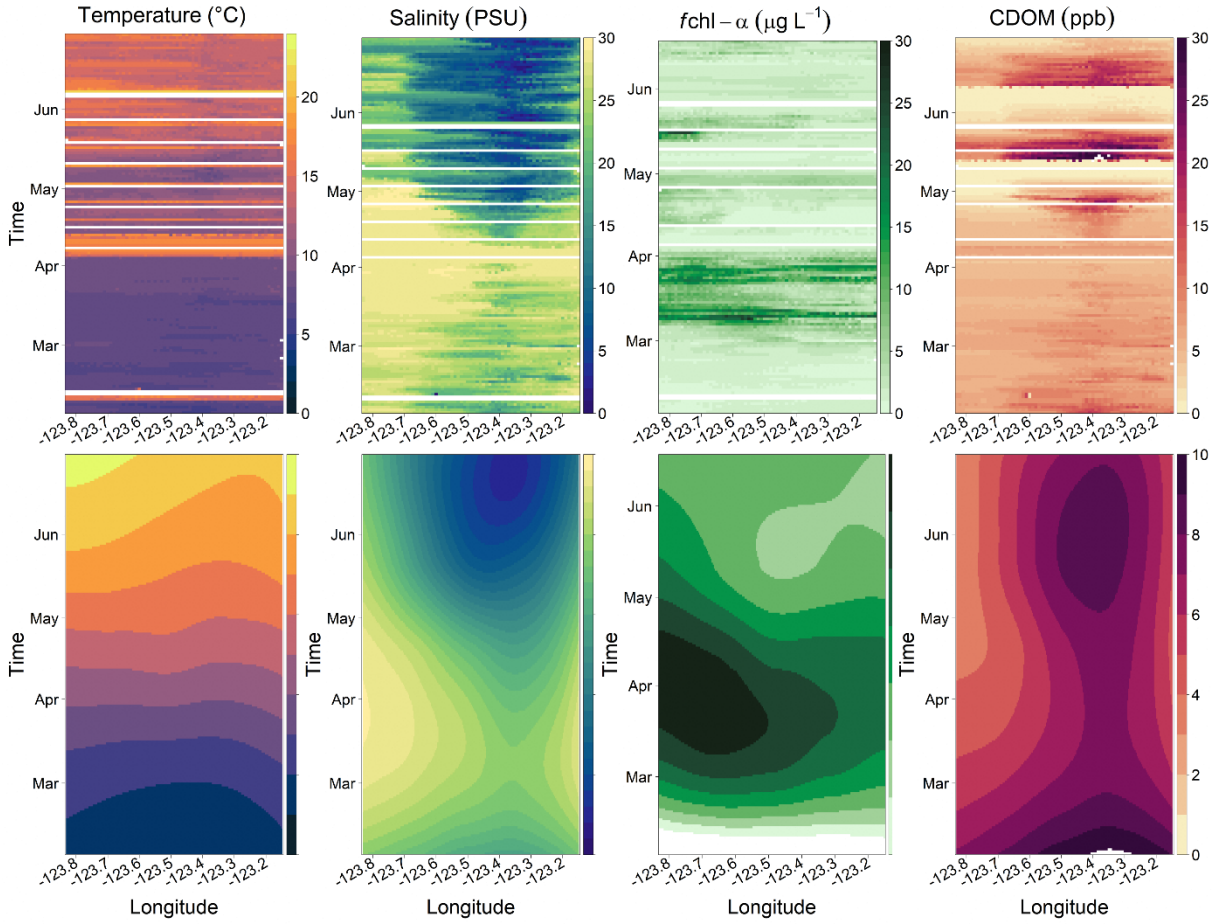

Figure S8. Hovmöller diagrams of FerryBox observations from February 01-June 30, 2020. Arranged spatiotemporally, the x-axis displays the cross-strait space (left to right: Duke Point to Tsawwassen) and the y-axis shows time. (Top row) Raw observations for each variable (in-vivo chlorophyll-α fluorescence, *f*chl-α; chromophoric dissolved organic matter, CDOM), where horizontal gaps represent sampling interruptions, displayed seasonality but contained high variation. (Bottom row) A loess-smoothing approximation captured general seasonal trends.

Literature Cited

Conway, D. V. P. (2006). Identification of the copepodite developmental stages of twenty-six North Atlantic copepods. Marine Biological Association of the United Kingdom. *21*, 28p.

Dancho, M. (2022). timetk: A Tool Kit for Working with Time Series, R package version 2.8.3, https://cran.r-project.org/web/packages/timetk/index.html.

Dolan, J. R. (2013). The Biology and Ecology of Tintinnid Ciliates: Models for Marine Plankton, First Edition. Montagnes, D. J. S., Agatha, S., Coats, D. W., Stoecker, D. K. John Wiley & Sons, Ltd. Published.

Garcia-Sucerquia, J., Ramırez, J. H., & Prieto, D. V. (2005). Improvement of the signal-to-noise ratio in digital holography. *Revista Mexicana De Fisica*. 51, 76–81.

Gómez, F. (2013). Reinstatement of the Dinoflagellate Genus *Tripos* to Replace *Neoceratium*, Marine Species of *Ceratium* (Dinophyceae, Aleolata). *CICIMAR Oceánides*, *28*(1), 1, https://doi.org/10.37543/oceanides.v28i1.119.

Hijmans, R. J. (2021). raster, R package version 3.6-14, https://cran.r-project.org/web/packages/raster/index.html.

Hasle, G.R., Syvertsen, E.E. (1997). Marine Diatoms. In: Tomas, C. R. (ed.) Identifying marine Phytoplankton. *Academic Press, Inc*., San Diego, p 5-385.

Kanka, M., Riesenberg, R., & Kreuzer, H. J. (2009). Reconstruction of high-resolution holographic microscopic images. *Optics Letters*, *34*(8), 1162. https://doi.org/10.1364/OL.34.001162.

Lamigueiro, O.P. (2022). rasterVis: Visualization Methods for Raster Data, R package version 0.51.5, https://cran.r-project.org/web/packages/rasterVis/index.html.

Owens, D., Abeysirigunawardena, D., Biffard, B., Chen, Y., and others. (2022). The Oceans 2.0/3.0 Data Management and Archival System. *Frontiers in Marine Science*, *9*, 806452. https://doi.org/10.3389/fmars.2022.806452.

Pebesma, E. (2018). Simple Features for R: Standardized Support for Spatial Vector Data. *The R Journal*, *10*(1), 439. https://doi.org/10.32614/RJ-2018-009.

R Core Team (2022). R: A language and environment for statistical computing. R Foundation for Statistical Computing, Vienna, Austria. URL https://www.R-project.org/.

Sakar, D., Andrews, F. (2022). latticeExtra: Extra Graphical Utilities Based on Lattice, R package version 0.6.29, https://cran.r-project.org/web/packages/latticeExtra/index.html.

Steidinger, K.A., Jangen, K. (1997). Dinoflagellates In: Tomas, C. R. (ed.) Identifying marine Phytoplankton. *Academic Press, Inc*., San Diego, p 387-584.

Throndsen, J. (1997). The planktonic marine flagellates. In: Tomas, C. R. (ed.) Identifying marine Phytoplankton. *Academic Press, Inc*., San Diego, p 591-730.

Walcutt, N. L., Knörlein, B., Cetinić, I., Ljubesic, Z., and others (2020). Assessment of holographic microscopy for quantifying marine particle size and concentration. *Limnology and Oceanography: Methods*, *18*(9), 516–530. https://doi.org/10.1002/lom3.10379

Wang, C., Pawlowicz, R., Sastri, A. R. (2019). Diurnal and Seasonal Variability of Near-Surface Oxygen in the Strait of Georgia. *Journal of Geophysical Research*: Oceans *124*, 2418–2439. https://doi.org/10.1029/2018JC014766

Wickham, H., Averick, M., Bryan, J., Chang, W., and others (2019). Welcome to the Tidyverse. *Journal of Open Source Software*, *4*(43), 1686. https://doi.org/10.21105/joss.01686.

Yin, K., Harrison, P. J., & Beamish, R. J. (1997). Effects of a fluctuation in Fraser River discharge on primary production in the central Strait of Georgia, British Columbia, Canada, *Canadian Journal of Fisheries and Aquatic Science*, *54*, 1015–1024.